
VideoCapsuleNet: A Simplified Network for Action Detection

Kevin Duarte
kevin_duarte@knights.ucf.edu

Yogesh S Rawat
yogesh@crcv.ucf.edu

Mubarak Shah
Center for Research in Computer Vision
University of Central Florida
Orlando, FL 32816
shah@crcv.ucf.edu

Abstract

The recent advances in Deep Convolutional Neural Networks (DCNNs) have shown extremely good results for video human action classification, however, action detection is still a challenging problem. The current action detection approaches follow a complex pipeline which involves multiple tasks such as tube proposals, optical flow, and tube classification. In this work, we present a more elegant solution for action detection based on the recently developed capsule network. We propose a 3D capsule network for videos, called VideoCapsuleNet: a unified network for action detection which can jointly perform pixel-wise action segmentation along with action classification. The proposed network is a generalization of capsule network from 2D to 3D, which takes a sequence of video frames as input. The 3D generalization drastically increases the number of capsules in the network, making capsule routing computationally expensive. We introduce *capsule-pooling* in the convolutional capsule layer to address this issue which makes the voting algorithm tractable. The routing-by-agreement in the network inherently models the action representations and various action characteristics are captured by the predicted capsules. This inspired us to utilize the capsules for action localization and the class-specific capsules predicted by the network are used to determine a *pixel-wise localization* of actions. The localization is further improved by parameterized skip connections with the convolutional capsule layers and the network is trained end-to-end with a classification as well as localization loss. The proposed network achieves state-of-the-art performance on multiple action detection datasets including UCF-Sports, J-HMDB, and UCF-101 (24 classes) with an impressive $\sim 20\%$ improvement on UCF-101 and $\sim 15\%$ improvement on J-HMDB in terms of v-mAP scores.

1 Introduction

Human action detection is a challenging computer vision problem, which involves detecting human actions in a long video as well as localizing these actions both spatially and temporally. In recent years, great progress have been achieved in solving action detection problem using deep learning methods Herath *et al.* (2017). Although the existing approaches have achieved a reasonable performance, these methods can be very complex. These networks tend to use multi-stage pipelines, which extract action proposals from a sequence of frames, classify these regions, and perform bounding box regressions on the proposals Hou *et al.* (2017); Gu *et al.* (2018); Kalogeiton *et al.* (2017). The two-stream networks Simonyan & Zisserman (2014); Carreira & Zisserman (2017) perform better

but they require computation and processing of optical flow. To overcome this drawback, we propose a simpler and more elegant solution to action detection through the use of capsules.

Capsule networks were introduced in Sabour *et al.* (2017) for the task of image classification. A capsule is a group of neurons which can model different entities or parts of entities. The capsules in a network undergo a routing-by-agreement algorithm which enables the capsule network to build parts-to-whole relationship between entities and allows capsules to learn viewpoint invariant representations. Through this improved representation learning, capsule networks are able to achieve state-of-the-art results in image domain with a drastic decrease in the number of parameters.

In this work, we aim at generalizing the capsule network from images to videos for the task of action detection. The proposed network, **VideoCapsuleNet**, uses 3D convolutions along with capsules to learn semantic information necessary for action detection. The predicted capsules can well capture the visual and motion characteristics of the input video clip which helps in action recognition. The network also has a localization component which utilizes the action representation captured by the capsules for a pixel-wise localization of actions. The capability of the capsules to learn meaningful representations of actions allows the localization network to predict fine pixel-wise segmentations of actions. VideoCapsuleNet is a much simpler network which can identify and localize actions in a given video, without the need of a region proposal network or optical flow information. Furthermore, it decreases the number of network parameters by using a simple encoder-decoder architecture, which takes a video clip as input and action localization and classification as an output and is trained end-to-end.

In summary, the main contribution of this work is the proposal of 3D capsule network to solve the problem of action detection in videos. To the best of our knowledge, this is the first work on capsules in the video domain. We present a novel *capsule-pooling* procedure for capsule routing, which greatly reduces the computational cost of routing in convolutional capsule layers. The network achieves state-of-the-art action localization results on the UCF-Sports, J-HMDB, and UCF-101 datasets with $\sim 15\text{-}20\%$ improvement on J-HMDB and UCF-101. Apart from action classification and pixel-wise localization, the predicted capsules in the network are also capable of explaining different characteristics of the action in the video.

2 Related Work

Action Detection The most successful action classification methods involve the use of CNNs Herath *et al.* (2017). Earlier deep learning works used CNNs to detect human actions in each frame and then stitch these detections to create spatio-temporal tubes Peng & Schmid (2016); Yang *et al.* (2017). Simonyan *et al.* Simonyan & Zisserman (2014) use a two-stream (spatial and temporal) CNN which processes a single frame along with multiple optical flow frames. Although the use of the temporal stream exploits motion in the video and improves accuracy, it requires a separate optical flow computations for each video. 3D CNNs Tran *et al.* (2015) have been shown to successfully extract spatio-temporal features, which can be used for action classification. The 3D kernels allow the CNN to learn temporal/motion information directly from the video frames. More recently, Carreira & Zisserman (2017) propose a two-stream I3D network which take advantage of ImageNet pretraining by inflating 2D ConvNets into 3D.

Approaches for action detection require networks to not only classify actions, but also localize them. Kalogeiton *et al.* Kalogeiton *et al.* (2017) use 2D CNNs to extract frame-level features and create action proposals through the use of anchor cuboids. These cuboids are then classified and refined through regression. Similarly, the TCNN Hou *et al.* (2017) use anchor boxes to create tube proposals, which are linked together and classified. The baseline presented in Gu *et al.* (2018) extends the I3D network for action localization by having a region proposal network that selects spatio-temporal regions to be classified and refined. Although the existing works shows promising results, all these approaches require complex region proposal networks that extract and classify spatio-temporal regions. As the complexity of these networks increase, it becomes more difficult to optimize the large number of parameters.

Capsules Sabour *et al.* Sabour *et al.* (2017) presented a capsule as a vector of neurons, whose orientation represents the properties of the entity and whose length represents the entity's existence. The routing algorithm measures agreement through a scalar product between two capsule vectors.

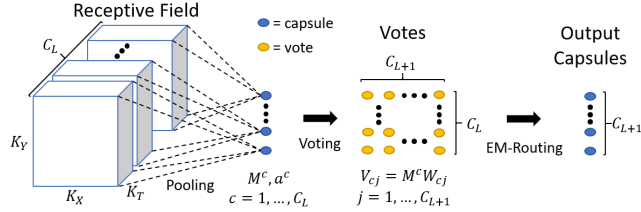


Figure 1: Capsule Pooling. New capsules are created by averaging the capsules in the receptive field for each capsule type. These new capsules then undergo the voting and routing-by-agreement procedure to obtain the capsules for the following layer.

In Hinton *et al.* (2018), Hinton et al. separate a capsule into a 4×4 pose matrix and an activation probability, to model the properties and existence of entities. The routing-by-agreement was replaced by a modified EM-algorithm which can better model the agreement between capsules. For the proposed VideoCapsuleNet, we use the capsules and routing algorithm similar to Hinton *et al.* (2018). In both of above works, the capsule networks were applied to images no larger than 32×32 . When dealing with larger images, or in this case videos of size $8 \times 112 \times 112$, routing of capsules become computationally expensive. We address this issue by implementing a mean-voting procedure in convolutional capsule layers (explained in section 3.1).

3 Generalizing capsules to higher dimensional inputs

For human action detection in videos, it is necessary to have a large enough network to successfully model the high dimensional data. Capsule transformation and routing is computationally expensive as compared with conventional convolutions and pooling. This makes generalization of capsule network to 3D very challenging. Therefore, it is crucial to optimize the routing procedure when scaling capsule networks to high dimensional inputs like videos.

A capsule is composed of a 4×4 pose matrix, M , and an activation probability, a Hinton *et al.* (2018). The pose matrix contains the instantiation parameters, or properties, of the entity, which it models and the activation probability is a scalar between 0 and 1, which represents the existence of the entity. The transformation matrix, W_{ij} , is used by a capsule i in layer L to cast a vote, $V_{ij} = M_i W_{ij}$, employing the pose matrix M_j of a capsule j in layer $L + 1$. The votes from all capsules in layer L are then used in an EM routing procedure to obtain the pose matrices and activation probabilities of the capsules in layer $L + 1$. Let N be the number of capsules in layer L , then the routing between layers L and $L + 1$ requires $N_L \times N_{L+1}$ votes to be computed. When the number of capsules in any layer becomes too large, the routing procedure becomes computationally intractable.

Convolutional Capsule Routing Convolutional capsules reduce the number of routed capsules by only computing votes for capsules within a local receptive field. In this case, the number of votes that undergo routing is proportional to the receptive field’s volume times the number of capsule types. However, this is not enough to reduce the computational cost if (i) the kernel/receptive field volume is large, as in our case when using 3-dimensional kernels, or (ii) the spatial/temporal dimensions of the convolutional capsule layer is large. In the previous 2-D capsule works for images, this is not an issue as the dimensions of the convolutional capsule layers are no larger than 14×14 and 3×3 kernels are used. When dealing with videos, these dimensions must be much larger: our first convolutional capsule layer has the dimensions $6 \times 20 \times 20$ and each capsule in the following capsule layer has a receptive field of $3 \times 5 \times 5$.

3.1 Capsule-Pooling

We propose a new voting procedure for convolutional capsule layers to reduce the number of computations used in capsule routing. First, we share transformation matrices between capsules of the same type; since capsules of the same type model the same entity at different positions, their votes should not vary based on their position. This decreases the number of learned parameters, which reduces the computation needed for the backward pass during training. Next, we reduce the number of votes being routed, by only applying the transformation matrix on the *mean* of the capsules in the receptive field of each capsule type.

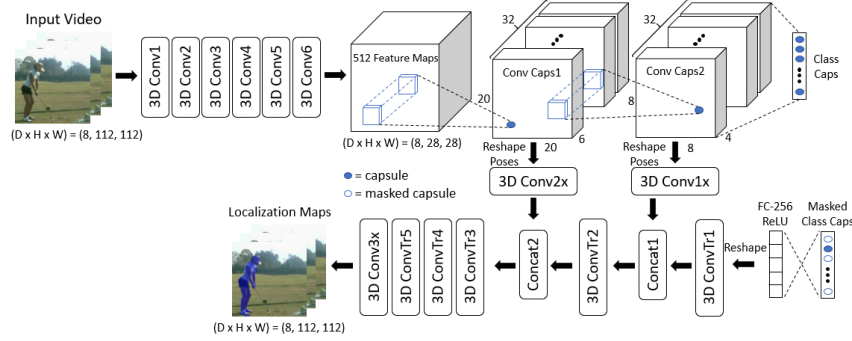


Figure 2: The VideoCapsuleNet Architecture. Features are extracted from the input frames by using 3D convolutions. These features are used to create the first capsule layer Conv Caps1. This is then followed by a convolutional capsule layer Conv Caps2 and then a fully connected capsule layer Class Caps. The decoder network uses the masked class capsules, skip connections from the convolutional capsule layers, and transposed convolutions to produce the pixel-wise action localization maps.

More formally, consider convolutional capsule routing between two layers, L and $L + 1$, where C is the number of capsule types in a layer. For 3D convolutional capsules, the receptive field of the capsules in layer $L + 1$ has the shape (K_T, K_X, K_Y) . In conventional convolutional capsule routing, each capsule in the receptive field would cast C_{L+1} votes, resulting in $C_L \times C_{L+1} \times K_T \times K_X \times K_Y$ votes for the routing procedure at each spatio-temporal position of layer $L + 1$. Since capsules of the same type model the same entity at different positions, we can safely assume that capsules of the same type that are close to each other should have similar poses and activations. Therefore, using the same transformation matrix on each capsule within a local receptive field would result in similar votes. This means that $K_T \times K_X \times K_Y$ similar votes are calculated $C_L \times C_{L+1}$ times. Each of these similar votes adds little useful information to the routing algorithm, making them redundant and unnecessary to compute. Instead of computing these redundant votes, we implement a capsule-pooling procedure as shown in Figure 1. For each capsule type, c , in layer L , we create one capsule with a pose matrix M^c and an activation a^c as follows:

$$M^c = \frac{1}{K_T K_X K_Y} \sum_{k=1}^{K_T} \sum_{i=1}^{K_X} \sum_{j=1}^{K_Y} M_{kij}^c, \quad a^c = \frac{1}{K_T K_X K_Y} \sum_{k=1}^{K_T} \sum_{i=1}^{K_X} \sum_{j=1}^{K_Y} a_{kij}^c, \quad (1)$$

where M_{kij}^c and a_{kij}^c are the pose matrix and activation of the capsule at position (k, i, j) in the receptive field. Now, each one of these capsules casts a vote for each capsule type in the layer $L + 1$, resulting in a total of $C_L \times C_{L+1}$ votes. Thus, capsule-pooling ensures we do not compute many similar votes; it ensures that the number of votes is only proportional to the number of capsule types in each layer, and indifferent to the volume of the receptive field.

4 Network Architecture

The VideoCapsuleNet architecture is shown in Figure 2. The input to the network is $8 \times 112 \times 112$ frames from a video. The network begins with $6 \times 3 \times 3 \times 3$ convolutional layers (each with ReLU activations) which result in 512 feature maps of dimension $8 \times 28 \times 28$. The first capsule layer is composed of 32 capsule types. The capsule 4×4 pose matrices and activations are obtained by applying a $3 \times 9 \times 9$ convolution operation, with ReLU and sigmoid activations respectively, to these 512 feature maps. This is followed by a second convolutional capsule layer with 32 capsule types, a $3 \times 5 \times 5$ receptive field, and a stride of $1 \times 2 \times 2$.

This second, and final, convolutional capsule layer is then fully connected to C capsules, where C is the number of action classes. For this final classification layer (class capsules), the capsule with the largest activation corresponds to the network’s action prediction. When computing the votes for this final convolutional capsule layer, all capsules of the same type share transformation matrices. In order to preserve the information about the convolutional capsules’ locations, we perform Coordinate Addition Hinton *et al.* (2018): at each position, we add the capsules’ coordinates (time, row, column) to the final three entries of the vote matrix.

Localization Network To obtain frame-level action localizations, we want to leverage the action-based representation found in the class capsule layer’s pose matrices. To this end we use the masking procedure as follows. During training we mask all pose matrices except for the one corresponding to the ground truth class, by setting their values to zero. At test time, all class capsules except the one with the largest activation, the predicted action, are masked. The class capsule poses are then fed into a fully connected layer which produces a $4 \times 8 \times 8$ feature map. This feature map corresponds to a rough localization of the action in the video. The localization is then upsampled through a series of transposed convolutions that result in $8 \times 112 \times 112$ localization maps. To ensure fine positional information is incorporated in this final localization, skip connections are used from the convolutional capsule layers; the pose matrices of these capsule layers are flattened and are used in a conventional convolution layer. Their outputs are then concatenated with the transposed convolution outputs.

4.1 Objective Function

VideoCapsuleNet is trained end-to-end using an objective function which is the sum of two losses: a classification loss and a localization loss. We use spread loss for classification which is computed as,

$$L_c = \sum_{i \neq t} \max(0, m - (a_t - a_i))^2, \quad (2)$$

where, a_i is the activation of the final class capsule corresponding to capsule i , and a_t is the target class’ activation. The margin m is linearly increased from 0.2 to 0.9 during training.

The network predicts a set of segmentation maps for action localization and sigmoid cross entropy is used to compute the loss. The shape of the network prediction is (T, X, Y) , where T corresponds to the temporal length, X corresponds to the height, and Y corresponds to the width of the prediction volume. The posterior probability of a pixel at position (k, i, j) of the predicted volume for an input video \hat{v} can be expressed as,

$$p_{kij} = \frac{e^{F_{kij}(\hat{v})}}{1 + e^{F_{kij}(\hat{v})}}, \quad (3)$$

where, F_{kij} is the activation value for pixel at position (k, i, j) of the predicted volume for an input video \hat{v} . The ground truth bounding box for a video is used to assign a actionness score (0 or 1) to each pixel position in the video. Let the ground truth actionness score of a pixel at position k, i, j in the input video \hat{v} is defined as \hat{p}_{kij} , then the cost function to be minimized for action localization is,

$$L_s = -\frac{1}{TXY} \sum_{k=1}^T \sum_{i=1}^X \sum_{j=1}^Y [\hat{p}_{kij} \log(p_{kij}) + (1 - \hat{p}_{kij}) \log(1 - p_{kij})]. \quad (4)$$

Thus, VideoCapsuleNet is trained using the objective function, $L = L_c + \lambda L_s$, where, λ is used to down-weight the localization loss so that it does not dominate the classification loss. In all experiments, we use $\lambda = 0.0002$.

5 Experiments

Implementation Details We implement VideoCapsuleNet using Tensorflow Abadi *et al.* (2016). For all experiments, the first 6 conv layers use C3D Tran *et al.* (2015) weights, pretrained on the Sports-1M Karpathy *et al.* (2014). The network was trained using the Adam optimizer Kingma & Ba (2014), with a learning rate of 0.0001. Due to the size of the VideoCapsuleNet, a batch size of 8 was used during training. We measure the performance of our network on three datasets UCF-Sports Rodriguez *et al.* (2008), J-HMDB Jhuang *et al.* (2013), UCF-101 Soomro *et al.* (2012). The only video preprocessing used is the downsampling of each video such that their shortest side is 120 px. We randomly crop 112x112 patches from 8 frame video during training and take a centre crop at test time. For UCF-Sports and UCF-101, we consider all pixels within the bounding box to be the ground-truth foreground while pixels outside of the bounding box are considered background. This results in more box-like segmentations, but in many cases VideoCapsuleNet produces tighter segmentations around the actor than the ground-truth bounding boxes (Figure 3).

Table 1: Action localization accuracy of VideoCapsuleNet. The results reported in the row VideoCapsuleNet* use the ground-truth labels when generating the localization maps, so they should not be directly compared with the other state-of-the-art results.

Method	UCF-Sports		J-HMDB		UCF-101				
	f-mAP	v-mAP	f-mAP	v-mAP	f-mAP	v-mAP			
	0.5	0.2	0.5	0.2	0.5	0.1	0.2	0.3	0.5
Saha et al. Saha <i>et al.</i> (2016)	-	-	-	72.6	-	76.6	66.8	55.5	35.9
Peng et al. Peng & Schmid (2016)	84.5	94.8	58.5	74.3	65.7	77.3	72.9	65.7	35.9
Singh et al. Singh <i>et al.</i> (2017)	-	-	-	73.8	-	-	73.5	-	46.3
Kalogeiton et al. Kalogeiton <i>et al.</i> (2017)	87.7	92.7	65.7	74.2	69.5	-	77.2	-	51.4
Hou et al. Hou <i>et al.</i> (2017)	86.7	95.2	61.3	78.4	67.3	77.9	73.1	69.4	-
Gu et al. Gu <i>et al.</i> (2018)	-	-	73.3	-	76.3	-	-	-	59.9
He et al. He <i>et al.</i> (2018)	-	96.0	-	79.7	-	-	71.7	-	-
VideoCapsuleNet	83.9	97.1	64.6	95.1	78.6	98.6	97.1	93.7	80.3
VideoCapsuleNet*	82.8	97.1	66.8	95.4	80.1	98.9	97.4	94.2	82.0

Metrics We compute frame-mAP and video-mAP for the evaluation Peng & Schmid (2016). For frame-mAP we set the IoU threshold at $\alpha = 0.5$, and compute the average precision over all the frames for each class. This is then averaged to obtain the f-mAP. For video-mAP the average precision is computed for the 3D IoUs at different thresholds over all the videos for each class, and then averaged to obtain the v-mAP.

5.1 Results

UCF-Sports and J-HMDB The UCF-Sports dataset consists of 150 videos from 10 action classes. All videos contain spatio-temporal annotations in the form of frame-level bounding boxes and we follow the standard training/testing split used by Lan *et al.* (2011). The J-HMDB dataset contains 21 action classes with a total of 928 videos. These videos have pixel-level localization annotations. Due to the size of these datasets, we pretrain the network using the UCF-101 videos, and fine-tune on their respective training sets. On UCF-Sports, we observe a slight improvement ($\sim 1\%$) in terms of v-mAP (Table 1). On J-HMDB, VideoCapsuleNet achieves a 15% improvement in v-mAP with a threshold of $\alpha = 0.2$ (Table 1). In both of these datasets, we find that we do not outperform the state-of-the-art when the f-mAP or v-mAP IoU thresholds are large. We attribute this to the small number of training videos per class (10 for UCF-Sports and 30 for J-HMDB). The f-mAP and v-mAP accuracy for different thresholds can be found in the supplementary file.

UCF-101 Our UCF-101 experiments are run on the 24 class subset consisting of 3207 videos with bounding box annotations provided by Singh *et al.* (2017). On UCF-101 VideoCapsuleNet outperforms existing methods in action localization, with a v-mAP accuracy 20% higher than the most state-of-the-art methods (Table 1). This shows that VideoCapsuleNet performs exceptionally well when the dataset is sufficiently large.

5.2 What class capsules learn?

Since all but one class capsule is masked out when the class capsules are passed to the localization network, each class capsule should contain localization information specific to their corresponding action (i.e. class capsule for *diving* should have information which would be useful when localizing the diving action). We found that this was indeed the case; at test time we masked all class capsules except the one corresponding to the ground-truth action, and localized the actions. These localization results can be found in Table 1 under VideoCapsuleNet*. When given the correct action to localize,

VideoCapsuleNet is able to improve its localizations. Figure 4 shows several examples of localizations, when different class capsules are masked.

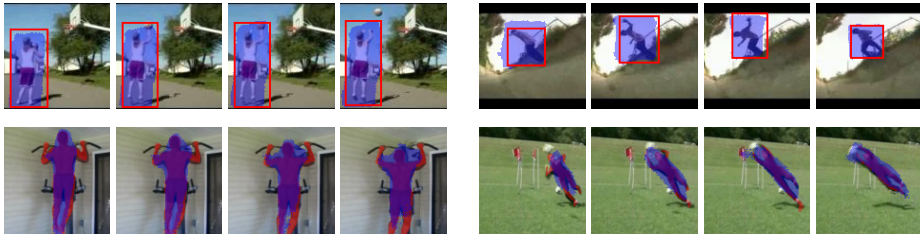


Figure 3: Sample action localizations for UCF-101 and J-HMDB. The UCF-101 videos have bounding box annotations (shown in red) and the predicted localizations are in blue. J-HMDB has pixel-wise annotations (shown in red) and the predicted localizations are in blue.

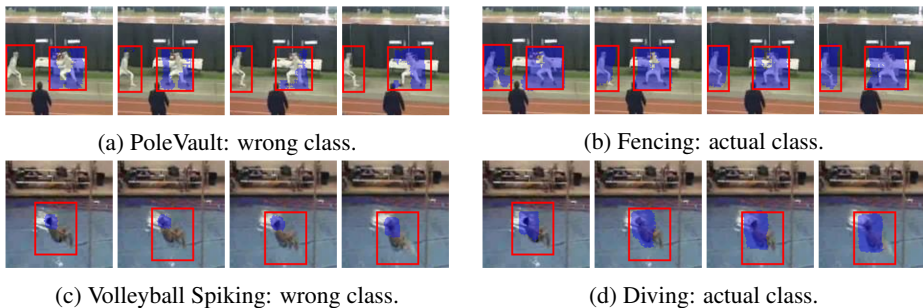


Figure 4: Sample localizations for UCF-101 videos (ground truth is red bounding box). The localizations on the left mask out all class capsules except the one corresponding to an incorrect action; the localizations on the right mask all capsules except the one corresponding to the correct (ground-truth) action. These localizations show that the class capsules contain action specific information and this information propagates to the localizations.

5.3 Ablation Experiments

Video Reconstructions Reconstruction can act as a regularizer in network training Sabour *et al.* (2017). To this end, we perform two experiments where the network reconstructs the original video; we add a convolutional layer to 3D ConvTr5, that has 3 channel outputs to reconstruct the input video. In the first experiment, the network is trained using the sum of the classification, localization, and reconstruction losses. In the second experiment the network is trained with only the classification and reconstruction losses. These experiments show us that the addition of a reconstruction network, when no localization information are available, do help the capsules learn better representations: there is a 10% increase in performance. However, localization information allows the capsules to learn better representations, allowing for improved classification performance. Using both the reconstruction and localization losses decrease the classification performance. We believe this additional loss forces the capsules to learn non-semantic information (RGB values), which hurts its ability to learn from the highly semantic bounding-box annotations.

Additional Skip Connections Due to first 6 convolutional layers (two of which have strides of 2 in the spatial dimensions) the network may lose some spatial information, we test the effectiveness of adding skip connections from these layers. For this experiment, we add skip connections at layers 3D Conv1, 3D Conv2, and 3D Conv4 to preserve the spatial information that is lost through striding. These additional skip connections result in similar classification and localization results as the base VideoCapsuleNet, but they increase the number of network parameters as well as the training time. For this reason, VideoCapsuleNet only has skip connections at the convolutional capsule layers.

Coordinate Addition Coordinate Addition allows the class capsules to encode positional information about the actions, which they represent, by adding the capsules’ coordinates (time, row, column)

Table 2: All ablation experiments are run on UCF-101. The f-mAP and v-mAP use IoU thresholds of $\alpha = 0.5$. (L_c :classification loss, L_s :localization loss, L_r : reconstruction loss, SC:skip connections, NCA:no coordinate addition, 4Conv:4 convolution layers, 8Conv: 8 convolution layers, and Full: the full network.) Unless specified, the network uses only the classification and localization losses.

	L_c	L_s	$L_c + L_r$	$L_c + L_s + L_r$	SC	NCA	4Conv	8Conv	Full
Accuracy	62.0	-	72.2	73.6	78.7	71.7	74.6	71.4	79.0
f-mAP	-	51.1	-	77.8	77.4	72.9	72.1	70.4	78.6
v-mAP	-	48.1	-	79.9	80.7	74.9	73.5	71.3	80.3

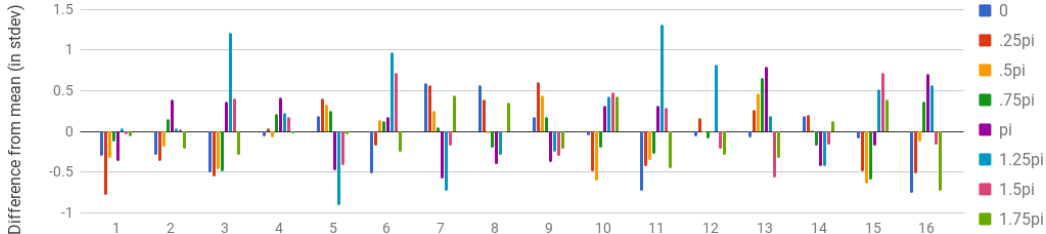


Figure 5: The 16 capsule dimensions of the Linear Motion pose matrix when the direction of motion is varied in synthetic videos. The direction 0: rightward movement, 0.25pi:diagonal movement (down and to the right), 0.5pi:downward movement. The rest of the directions follow this pattern (step of .25pi in angle). Most dimensions have a sinusoidal pattern as the direction of motion varies, which show that the pose matrix values change smoothly as video inputs change.

to the vote matrices of the final convolutional capsule layer. In our synthetic dataset experiments, we show that this is the case: these three capsule dimensions change predictably as the direction and speed of the motion change. This improved encoding improves the networks classification accuracy by about 7% and the localization accuracy by about 5% on the UCF-101 dataset.

5.4 Synthetic Dataset Experiments

We run several experiments on a synthetic video dataset to better understand the instantiation parameters encoded in the class capsules’ pose matrices. We use synthetic data (more details in supplementary file), since they allow us to control specific properties of the videos, which would be difficult to do with real-world videos. There are 4 action classes which corresponds to different types of motion: linear, circular, a turn, and random. VideoCapsuleNet is trained on these randomly generated videos, and then we measure the dimensions of the class capsules’ pose matrices when varying different properties of the generated videos.

We found that VideoCapsuleNet’s class capsules are able to parameterize the different visual and motion properties in video. Since the network uses Coordinate Addition, the final three dimensions of the pose matrices contains information about the actor’s position. As we linearly increase the object’s speed in the video, the dimension corresponding to the time coordinate increases in a linear fashion. Similarly, the dimensions corresponding to the row and column coordinates changes as the direction of the motion changed: vertical motion changed the dimensions corresponding to the row; horizontal motion changes the dimension corresponding to the column. This change is illustrated in the last two dimensions of Figure 5. Interestingly, these are not the only dimensions which smoothly change as the direction or speed change. Almost all capsule dimensions, for the linear motion class capsule, change smoothly as different properties (size, direction, speed, etc.) change in the video.

Since the dimensions do not change in an arbitrary fashion as the inputs change, VideoCapsuleNet’s class capsules successfully encode the visual and motion characteristics of the actor. This helps explain why VideoCapsuleNet is able to achieve such good localization results; the capsules learn to represent the different spatio-temporal properties necessary for accurate action localizations.

5.5 Computational Cost and Training Speed

Although capsule networks tend to be computationally expensive (due to the routing-by-agreement), capsule-pooling allows VideoCapsuleNet to run on a single Titan X GPU using a batch size of 8. Also, VideoCapsuleNet trains quickly when compared to other approaches: on UCF-101 it converges

in fewer than 120 epochs, or 34.5K iterations. This is substantially fewer iterations than the 70K iterations for Peng & Schmid (2016), 100K iterations for the TCNN Hou *et al.* (2017), 600K-1M iterations for Gu *et al.* (2018).

6 Conclusion and Future Work

In this work we propose VideoCapsuleNet, a 3D generalization of capsule network from 2D images to 3D videos, for action detection. To the best of our knowledge, this is the first work where capsules are employed for videos. The proposed network takes video frames as input and predicts an action class as well as a pixel-wise localization for the input video clip. We introduce capsule-pooling to optimize the voting algorithm in the convolutional capsule layers which makes the routing feasible. The proposed network has a localization component which generates pixel-wise localization considering the predicted class-specific capsules. VideoCapsuleNet can be trained end-to-end and we obtain state-of-the-art performance on multiple action detection datasets. Research on capsules is still at an initial stage and we have already seen some good performances on different tasks. The basic idea behind capsule is very intuitive and there are many fundamental reasons, which makes capsules a better approach than conventional ConvNets, however, it will require a lot more effort to fully validate these facts. The results we have achieved in this paper on videos are promising and indicate the potential of capsules for videos which makes it worth exploring.

References

- Abadi, Martín, Barham, Paul, Chen, Jianmin, Chen, Zhifeng, Davis, Andy, Dean, Jeffrey, Devin, Matthieu, Ghemawat, Sanjay, Irving, Geoffrey, Isard, Michael, *et al.* . 2016. TensorFlow: A System for Large-Scale Machine Learning. *Pages 265–283 of: OSDI*, vol. 16.
- Carreira, Joao, & Zisserman, Andrew. 2017. Quo vadis, action recognition? a new model and the kinetics dataset. *Pages 4724–4733 of: 2017 IEEE Conference on Computer Vision and Pattern Recognition (CVPR)*. IEEE.
- Gu, Chunhui, Sun, Chen, Vijayanarasimhan, Sudheendra, Pantofaru, Caroline, Ross, David A, Toderici, George, Li, Yeqing, Ricco, Susanna, Sukthankar, Rahul, Schmid, Cordelia, *et al.* . 2018. AVA: A video dataset of spatio-temporally localized atomic visual actions. *CVPR*.
- He, Jiawei, Ibrahim, Mostafa S, Deng, Zhiwei, & Mori, Greg. 2018. Generic Tubelet Proposals for Action Localization. *WACV*.
- Herath, Samitha, Harandi, Mehrtash, & Porikli, Fatih. 2017. Going deeper into action recognition: A survey. *Image and vision computing*, **60**, 4–21.
- Hinton, Geoffrey E, Sabour, Sara, & Frosst, Nicholas. 2018. Matrix capsules with EM routing. *In: International Conference on Learning Representations*.
- Hou, Rui, Chen, Chen, & Shah, Mubarak. 2017. Tube convolutional neural network (T-CNN) for action detection in videos. *In: IEEE International Conference on Computer Vision*.
- Jhuang, Hueihan, Gall, Juergen, Zuffi, Silvia, Schmid, Cordelia, & Black, Michael J. 2013. Towards understanding action recognition. *Pages 3192–3199 of: Computer Vision (ICCV), 2013 IEEE International Conference on*. IEEE.
- Kalogeiton, Vicky, Weinzaepfel, Philippe, Ferrari, Vittorio, & Schmid, Cordelia. 2017. Action tubelet detector for spatio-temporal action localization. *In: ICCV-IEEE International Conference on Computer Vision*.
- Karpathy, Andrej, Toderici, George, Shetty, Sanketh, Leung, Thomas, Sukthankar, Rahul, & Fei-Fei, Li. 2014. Large-scale video classification with convolutional neural networks. *Pages 1725–1732 of: Proceedings of the IEEE conference on Computer Vision and Pattern Recognition*.
- Kingma, Diederik P, & Ba, Jimmy. 2014. Adam: A method for stochastic optimization. *arXiv preprint arXiv:1412.6980*.
- Lan, Tian, Wang, Yang, & Mori, Greg. 2011. Discriminative figure-centric models for joint action localization and recognition. *Pages 2003–2010 of: Computer Vision (ICCV), 2011 IEEE International Conference on*. IEEE.

- Peng, Xiaojiang, & Schmid, Cordelia. 2016. Multi-region two-stream R-CNN for action detection. *Pages 744–759 of: European Conference on Computer Vision*. Springer.
- Rodriguez, Mikel D, Ahmed, Javed, & Shah, Mubarak. 2008. Action mach a spatio-temporal maximum average correlation height filter for action recognition. *Pages 1–8 of: Computer Vision and Pattern Recognition, 2008. CVPR 2008. IEEE Conference on*. IEEE.
- Sabour, Sara, Frosst, Nicholas, & Hinton, Geoffrey E. 2017. Dynamic routing between capsules. *Pages 3859–3869 of: Advances in Neural Information Processing Systems*.
- Saha, Suman, Singh, Gurkirt, Sapienza, Michael, Torr, Philip HS, & Cuzzolin, Fabio. 2016. Deep learning for detecting multiple space-time action tubes in videos. *BMVC*.
- Simonyan, Karen, & Zisserman, Andrew. 2014. Two-stream convolutional networks for action recognition in videos. *Pages 568–576 of: Advances in neural information processing systems*.
- Singh, Gurkirt, Saha, Suman, Sapienza, Michael, Torr, Philip, & Cuzzolin, Fabio. 2017. Online Real time Multiple Spatiotemporal Action Localisation and Prediction.
- Soomro, Khurram, Zamir, Amir Roshan, & Shah, Mubarak. 2012. UCF101: A dataset of 101 human actions classes from videos in the wild. *arXiv preprint arXiv:1212.0402*.
- Tran, Du, Bourdev, Lubomir, Fergus, Rob, Torresani, Lorenzo, & Paluri, Manohar. 2015. Learning spatiotemporal features with 3d convolutional networks. *Pages 4489–4497 of: Computer Vision (ICCV), 2015 IEEE International Conference on*. IEEE.
- Yang, Zhenheng, Gao, Jiyang, & Nevatia, Ram. 2017. Spatio-Temporal Action Detection with Cascade Proposal and Location Anticipation. *BMVC*.

Appendix A Synthetic dataset experiments

For the synthetic dataset, there are 4 action classes which corresponds to different types of motion: linear motion, circular motion, a turn motion, and random motion. The properties that vary in all videos are the shape (circle, square, or triangle), shape size, color, speed (constant or accelerating), direction, amount of noise, rotation, and zooming in/out. Figure 1 shows some examples of the video clips generated for this dataset. VideoCapsuleNet is trained on about 200,000 randomly generated videos until the loss is minimized on a hold-out set of 2000 videos (500 from each class). On this hold-out set, the network is able to achieve 90% accuracy.

Most analysis was done on the class capsule for linear motion. To find the "average" value of the pose matrix for linear motion, we randomly generate 20,000 linear motion videos and make the network classify them. We then find the mean μ_d and standard deviation σ_d for each pose matrix dimension (only using the values obtained when the network correctly classifies the action). Then, we can generate 500 different linear motion videos with specific properties (i.e. a specific speed, a specific direction...) and calculate the mean μ'_d of the capsule's dimensions for these videos. With this, we can see how this specific change effected the pose matrix dimensions by calculating $\frac{\mu_d - \mu'_d}{\sigma_d}$.

We found that the capsule's pose matrix encodes the speed, direction, size, and rotation. The following figures (Figures 2-5) show the changes in the capsule dimensions as different properties of the video are changes. Nearly all dimensions smoothly change as the various video properties change, which means that the capsule successfully encodes the instantiation parameters of the actor/video.

Appendix B Localization Results at different thresholds

Here we present the localization results for VideoCapsuleNet on the three datasets (UCF-Sports, J-HMDB, and UCF-101) in Tables 1, 2, and 3. We find that our network outperforms state-of-the-art networks on all three datasets when the IoU threshold is small. However, for the smaller datasets (UCF-Sports and J-HMDB) we find that VideoCapsuleNet slightly under-performs when the v-mAP IoU threshold becomes larger (>0.4). We attribute this to the lack of training data for each class in these datasets (10 videos per class in UCF-Sports, and 30 videos per class in J-HMDB). This is supported by the fact that VideoCapsuleNet achieves outstanding results at nearly all IoU thresholds on UCF-101 which has about 100 videos per class in the training set. As action detection datasets become larger, it would be interesting to see how VideoCapsuleNet's accuracy scales with the increase of training samples.

Appendix C Class-wise Localizations

We show the frame average precision and video average precision for each class of J-HMDB and UCF-101 in Tables 4 and 5. In J-HMDB, the network produces poor localizations for the "Push" and "Jump" actions. Both of these actions have very different backgrounds, which could be an explanation

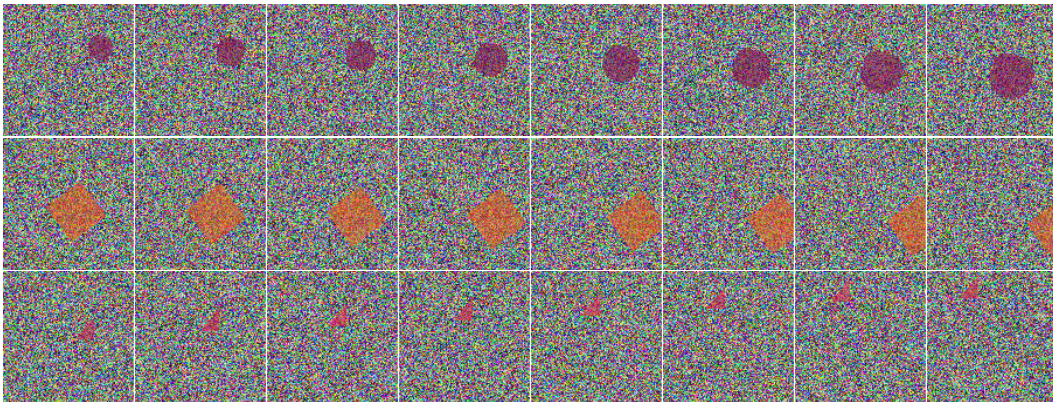


Figure 6: Sample video clips generated for the synthetic dataset.

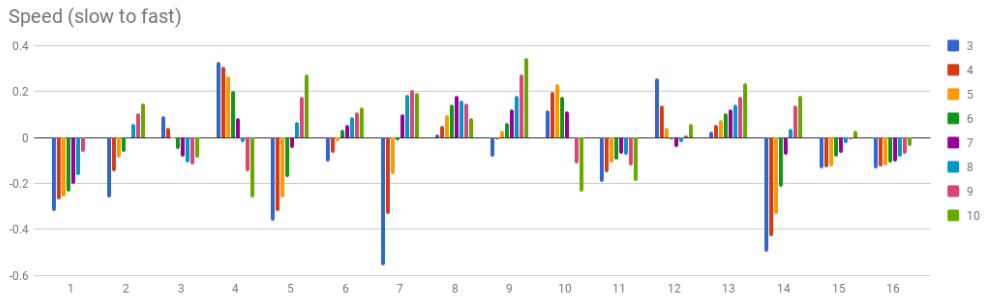


Figure 7: The 16 capsule dimensions of the Linear Motion pose matrix when the speed varies.

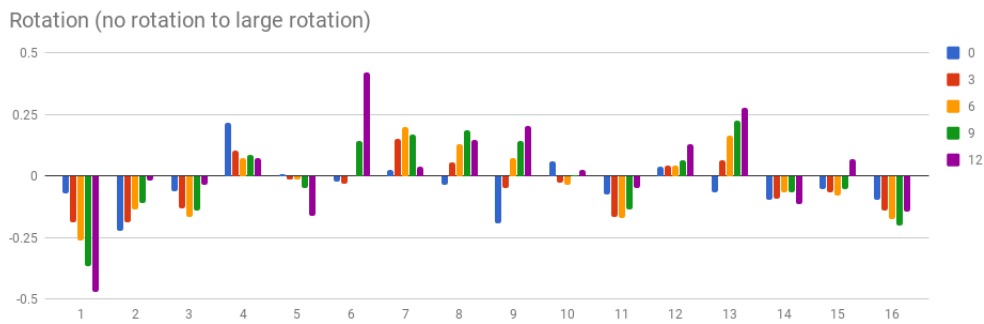


Figure 8: The 16 capsule dimensions of the Linear Motion pose matrix when the rotation varies.

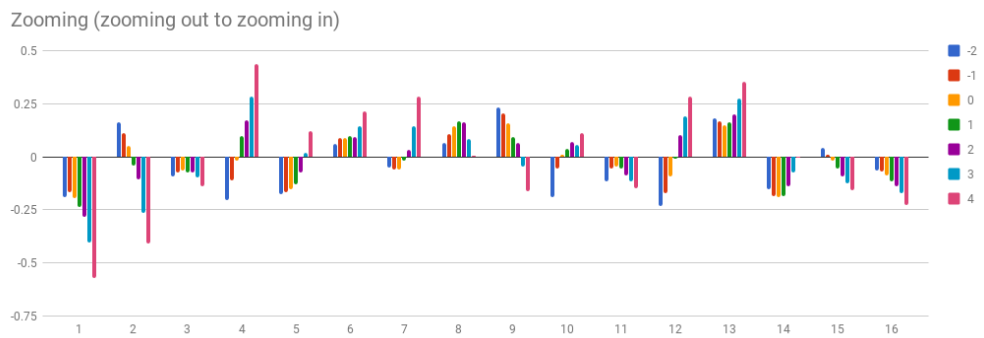


Figure 9: The 16 capsule dimensions of the Linear Motion pose matrix when the video zooms in and out.

Table 3: UCF-Sports Localization Results at different thresholds.

IoU Threshold	f-mAP	v-mAP
0.05	97.46	98.57
0.10	96.55	98.57
0.15	96.11	97.14
0.20	95.35	97.14
0.25	94.68	97.14
0.30	93.76	97.14
0.35	92.37	92.12
0.40	89.49	92.12
0.45	86.98	89.05
0.50	83.91	84.88
0.55	79.55	82.38
0.60	73.70	79.88
0.65	67.38	70.71
0.70	58.59	60.12
0.75	46.68	28.45
0.80	31.17	20.36
0.85	11.73	9.76
0.90	5.97	0.00
0.95	0.47	0.00

Table 4: J-HMDB Localization Results at different thresholds.

IoU Threshold	f-mAP	v-mAP
0.05	97.09	99.19
0.10	95.71	98.41
0.15	94.28	96.97
0.20	92.56	95.13
0.25	90.21	93.21
0.30	86.93	89.08
0.35	82.95	85.11
0.40	77.83	79.32
0.45	71.82	70.56
0.50	64.63	61.95
0.55	55.41	52.59
0.60	43.39	38.65
0.65	28.96	23.72
0.70	15.11	10.28
0.75	5.83	3.01
0.80	1.24	0.46
0.85	0.08	0.00
0.90	0.00	0.00
0.95	0.00	0.00

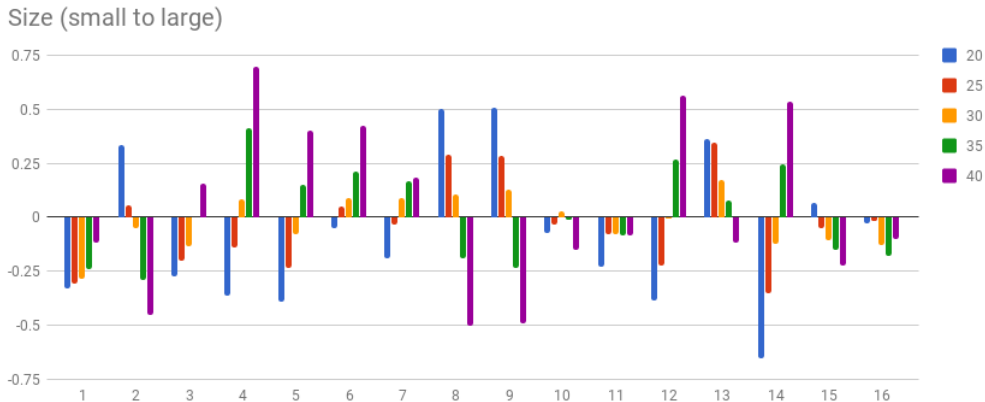


Figure 10: The 16 capsule dimensions of the Linear Motion pose matrix when the size varies.

Table 5: UCF101 Localization Results at different thresholds.

IoU Threshold	f-mAP	v-mAP
0.05	93.96	99.16
0.10	93.16	98.59
0.15	92.28	97.86
0.20	91.35	97.09
0.25	90.24	95.67
0.30	88.84	93.71
0.35	87.02	91.56
0.40	84.78	89.53
0.45	82.08	85.55
0.50	78.59	80.25
0.55	73.78	74.85
0.60	67.76	67.06
0.65	59.82	56.81
0.70	49.75	42.45
0.75	38.10	26.12
0.80	25.07	12.15
0.85	12.33	2.26
0.90	3.30	0.00
0.95	0.17	0.00

for these results. In UCF-101, we see that the network performs worst on the "BasketballDunk" and "VolleyballSpiking" actions. The videos for both of these classes involve many humans, one of which is performing the action, so the network often classifies multiple humans as foreground actors.

Appendix D More Qualitative Results

Figure 6 shows VideoCapsuleNet’s localizations on the UCF-101 and J-HMDB datasets. On the UCF-101 dataset, which provides bounding-box annotations, we find that the VideoCapsuleNet produces box-like action segmentations. However, it is sometimes able to produce localizations which contour better to the actor’s limbs, even though pixel-level action segmentations are not given.

When fine-tuned to the J-HMDB dataset (which has pixel-level annotations), we see that these box-like segmentations become more form-fitting. However, we do see that VideoCapsuleNet is unable to perfectly capsule the actor’s arms, and often localizes the larger parts of the actor (the torso and legs). We can attribute this to the 112x112 frame size, which makes these arms only a few pixels thick. It can be seen in the baby clapping example (row 6 in figure 6) that the network does adjust the width of the localization as the baby’s hands come closer together.

Table 6: J-HMDB Class-wise Localization Results at threshold $\alpha = 0.5$.

Class	f-AP	v-AP
BrushHair	71.39	69.44
Catch	79.81	76.35
Clap	70.72	79.49
ClimbStairs	66.75	72.22
Golf	94.71	97.22
Jump	30.43	14.44
KickBall	67.68	70.40
Pick	60.43	58.33
Pour	61.28	64.58
Pullup	80.87	85.42
Push	22.34	16.67
Run	67.88	59.09
ShootBall	62.57	62.88
ShootBow	92.90	93.33
ShootGun	56.93	53.61
Sit	50.93	42.93
Stand	46.66	36.36
SwingBaseball	94.93	97.92
Throw	50.91	41.86
Walk	62.07	52.78
Wave	65.04	55.56

Table 7: UCF-101 Class-wise Localization Results at threshold $\alpha = 0.5$.

Class	f-AP	v-AP
Basketball	64.85	65.71
BasketballDunk	46.70	37.84
Biking	82.14	92.11
CliffDiving	56.02	46.15
CricketBowling	87.08	83.33
Diving	76.74	84.44
Fencing	83.53	94.12
FloorGymnastics	86.59	91.67
GolfSwing	89.80	84.62
HorseRiding	93.03	100.00
IceDancing	99.34	100.00
LongJump	65.20	65.79
PoleVault	62.13	65.00
RopeClimbing	91.55	97.06
SalsaSpin	97.56	100.00
SkateBoarding	87.97	100.00
Skiing	74.39	70.00
Skijet	71.52	71.43
SoccerJuggling	92.62	100.00
Surfing	73.29	72.73
TennisSwing	90.37	93.88
TrampolineJumping	83.14	93.88
VolleyballSpiking	47.21	33.33
WalkingWithDog	83.38	83.33

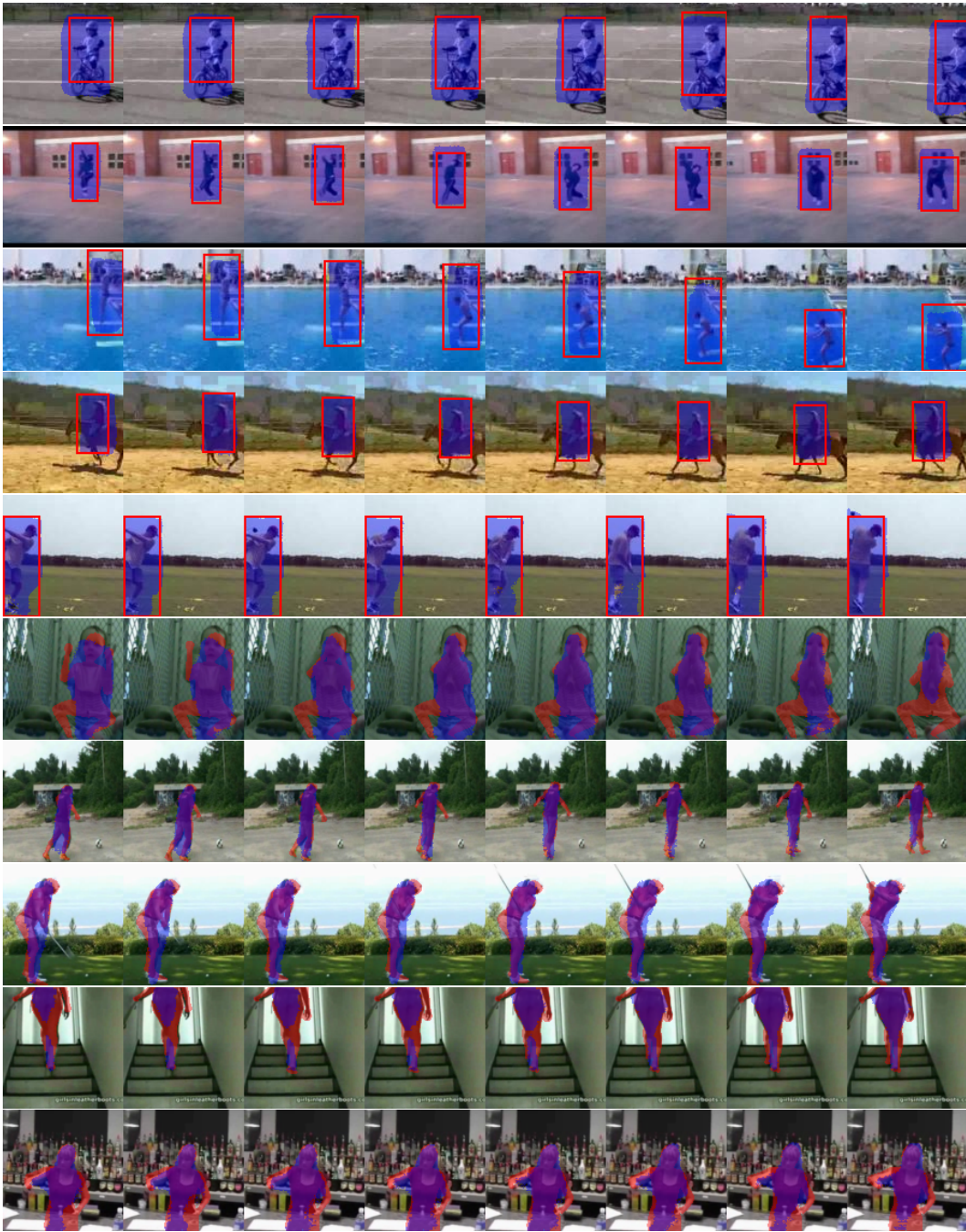


Figure 11: Sample localizations for UCF-101 and J-HMDB. The UCF-101 videos have bounding box annotations (shown in red) and the predicted localizations are in blue. J-HMDB has pixel-wise annotations (shown in red) and the predicted localizations are in blue.

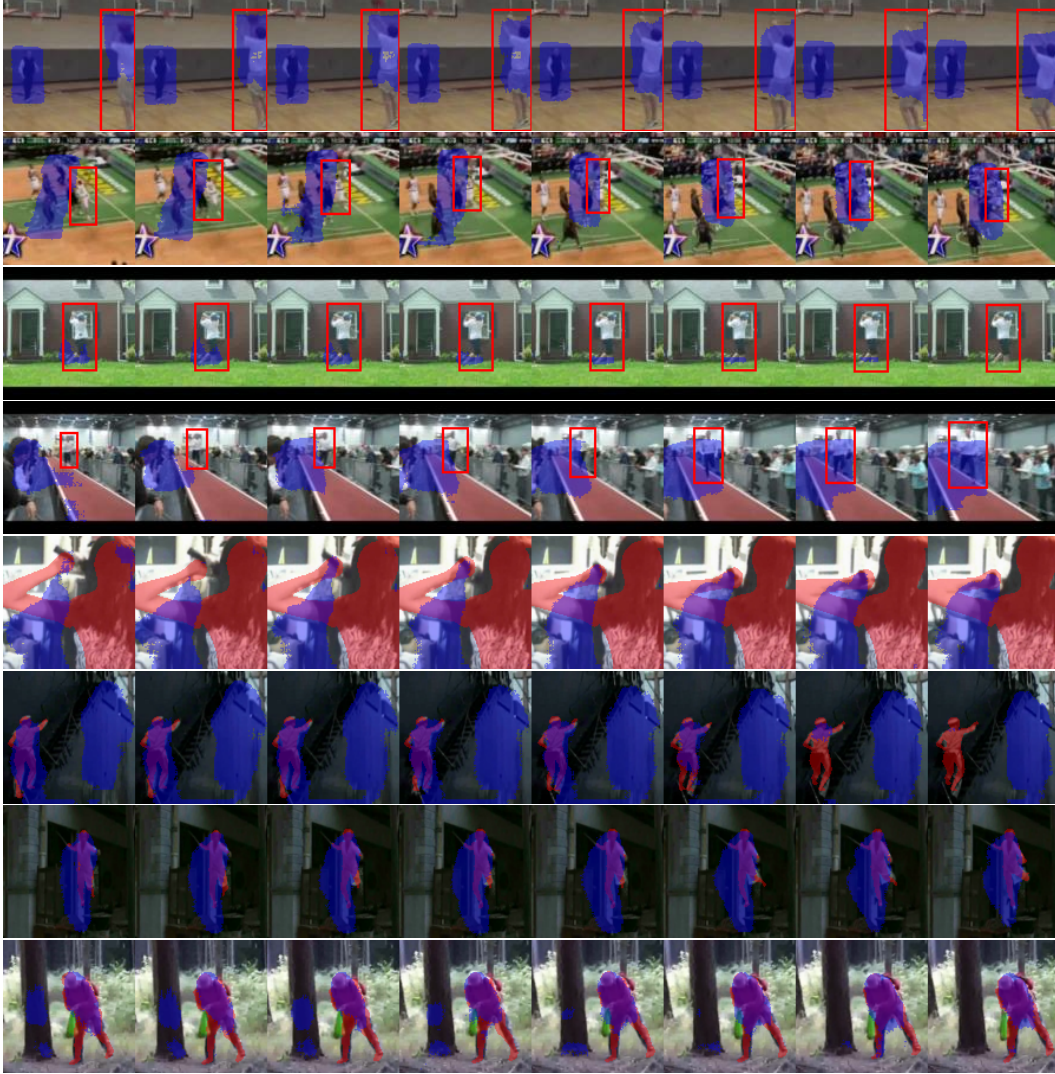


Figure 12: Sample failure cases for UCF-101 and J-HMDB. The UCF-101 videos have bounding box annotations (shown in red) and the predicted localizations are in blue. J-HMDB has pixel-wise annotations (shown in red) and the predicted localizations are in blue.

Appendix E Localization Failure Cases

Figure 7 shows some failure cases for VideoCapsuleNet on the UCF-101 and J-HMDB test data. One common failure case is when there are many humans in the video and there is only 1 actor. In these cases, the network labels several humans as the foreground, even though only one is considered the foreground. Another localization error that has been observed is the labeling the actor and large portions of the background as the foreground (as seen in the final three video localizations). This second type of error is usually accompanied by a miss-classification, which shows that the network is unable to understand these particular scenes.

Appendix F Network Parameters

Table 6 shows different layers of VideoCapsuleNet, and their different parameters.

Table 8: The specific network parameters. The layer names used correspond to those used in Figure 2 in the main text. Channels for capsule layers correspond to the number of capsule types in that layer.

Layer	Kernel Dims ($D \times H \times W$)	Strides ($D \times H \times W$)	Output Dims ($D \times H \times W \times C$)
3D Conv1	$3 \times 3 \times 3$	$1 \times 1 \times 1$	$8 \times 112 \times 112 \times 64$
3D Conv2	$3 \times 3 \times 3$	$1 \times 2 \times 2$	$8 \times 56 \times 56 \times 128$
3D Conv3	$3 \times 3 \times 3$	$1 \times 1 \times 1$	$8 \times 56 \times 56 \times 256$
3D Conv4	$3 \times 3 \times 3$	$1 \times 2 \times 2$	$8 \times 28 \times 28 \times 256$
3D Conv5	$3 \times 3 \times 3$	$1 \times 1 \times 1$	$8 \times 56 \times 56 \times 512$
3D Conv6	$3 \times 3 \times 3$	$1 \times 1 \times 1$	$8 \times 28 \times 28 \times 512$
Conv Caps1	$3 \times 9 \times 9$	$1 \times 1 \times 1$	$6 \times 20 \times 20 \times 32$
Conv Caps2	$3 \times 5 \times 5$	$1 \times 2 \times 2$	$4 \times 8 \times 8 \times 32$
Class Caps	-	-	N
FC-256 + Reshape	-	-	$4 \times 8 \times 8 \times 1$
3D ConvTr1	$1 \times 3 \times 3$	$1 \times 1 \times 1$	$4 \times 8 \times 8 \times 128$
3D Conv1x	$1 \times 3 \times 3$	$1 \times 1 \times 1$	$4 \times 8 \times 8 \times 128$
Concat1	-	-	$4 \times 8 \times 8 \times 256$
3D ConvTr2	$3 \times 6 \times 6$	$1 \times 2 \times 2$	$6 \times 20 \times 20 \times 128$
3D Conv2x	$1 \times 3 \times 3$	$1 \times 1 \times 1$	$6 \times 20 \times 20 \times 128$
Concat2	-	-	$6 \times 20 \times 20 \times 256$
3D ConvTr3	$3 \times 9 \times 9$	$1 \times 1 \times 1$	$8 \times 28 \times 28 \times 256$
3D ConvTr4	$1 \times 3 \times 3$	$1 \times 2 \times 2$	$8 \times 56 \times 56 \times 256$
3D ConvTr5	$1 \times 3 \times 3$	$1 \times 2 \times 2$	$8 \times 112 \times 112 \times 256$
3D Conv3x	$1 \times 3 \times 3$	$1 \times 1 \times 1$	$8 \times 112 \times 112 \times 1$